COMPREHENSIVE ACTIVE MICROVIBRATION CONTROL SYSTEM USING PIEZOELECTRIC ACTUATORS FOR BASE-ISOLATED PRECISION MANUFACTURING FACILITIES (PART II)

Mamoru SHIMAZAKI[1], Takafumi FUJITA[2], Yoshiyuki HASHIMOTO[3], Hirokazu YOSHIOKA[3], Takashi KITAHARA[4] and Tomohiro OGAWA[5]

ABSTRACT: Active microvibration control is expected to be applied to floors and even entire buildings of precision manufacturing facilities to meet requirements for more perfect vibration-free environment in the facilities. It is desirable that such facilities are effectively protected from earthquake attacks by using seismic isolation. For base-isolated precision manufacturing facilities, comprehensive active microvibration control systems were studied. The tests showed that the system consisting of the passive base-isolation system and the piezoelectric actuators attached to the columns and the beams could most effectively control the three-dimensional microvibrations due to the external and the internal disturbances.

Key Words: Microvibration, Active Control, Smart Structure, Piezoelectric Actuator, Precision Manufacturing Facility, Base-Isolation, Model Matching Method, Damping, Modal Analysis, Finite Element Method

INTRODUCTION

It is expected that the active microvibration control will be applied to floors and even entire buildings to meet requirements for more perfect vibration-free environment in precision manufacturing facilities [1]. Furthermore, particularly in Japan, it is desirable that such facilities are effectively protected from earthquake attacks by seismic isolation. Therefore, comprehensive active microvibration control systems will be required in such base-isolated precision manufacturing facilities, in order to control both of microvibrations born in the inside due to equipment and human walks and microvibrations coming from the outside due to ground vibrations and winds. In this study, a base-isolated 2-story building model of a $3m \times 5m \times 4m^{H}$ external size and a 6.9t total mass was used for experiments, in which four multistage rubber bearings and a viscous shear damper were installed for the seismic isolation, while 20 piezoelectric actuators were attached to the columns and the beams and eight piezoelectric actuator units were installed in the seismic isolation layer for the active control.

[1] Technical Associate, Institute of Industrial Science, The University of Tokyo
[2] Professor, Institute of Industrial Science, The University of Tokyo
[3] Takenaka Corporation
[4] Hitachi Plant Engineering & Construction Co., Ltd.
[5] Sumitomo Heavy Industries, Ltd.

EXPERIMENTAL MODEL

Figures 1 and 2 show a photograph and a schematic drawing of the building model used in the study respectively. The building model was a base-isolated 2-story steel frame structure of a $5\times3\times4^{H}$ m external size and a 6,900 kg total mass, in which four multistage rubber bearings and a viscous shear damper were installed for the seismic isolation. Figure 3 shows a schematic drawing of the viscous shear damper. In the building model, two shakers were installed in the center of the first floor to simulate the three-dimensional microvibrations generated by the machines in the building. Furthermore, another shaker was installed in the center of the roof floor to simulate the horizontal microvibrations excited by the wind.

As shown in figure 4, each column of the first story had a stage in its bottom part, and four piezoelectric actuators of a $25\times25\times36^{H}$ mm external size were installed in each stage to control the bending moment of the column in the two lateral directions. Each beam of the second floor in the longitudinal direction had a stage at its midpoint, and two piezoelectric actuators of the same size were installed in each stage to control the bending moment of the beam in the vertical direction. Figure 5 shows a installation method of the piezoelectric actuator.

Figure 6 shows a method for controlling the bending moment via piezoelectric actuators. Exactly before the control starts, the actuators on both sides of the column/beam are slightly lengthened by a bias input voltage. This state becomes the equilibrium state during the control. Then the actuators are lengthened or shortened with respect to the equilibrium state by a control voltage. Therefore, the actuators can push and pull the arms attached to the column/beam and can control the bending moments applied to the column/beam as shown in Fig. 6 [2].

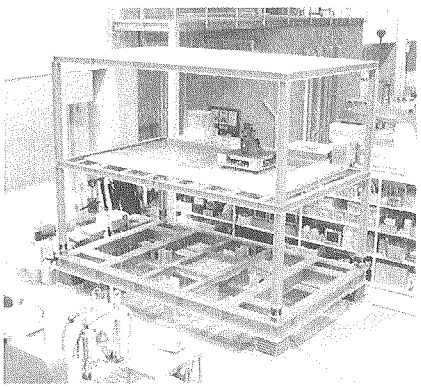

Figure 1 Building model

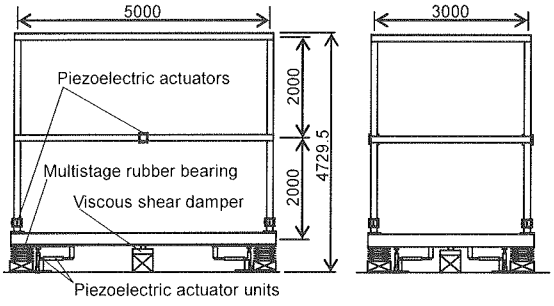

Figure 2 Schematic drawing of building model

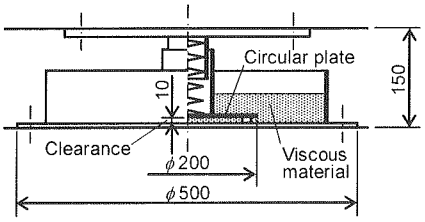

Figure 3 Schematic drawing of viscous shear damper

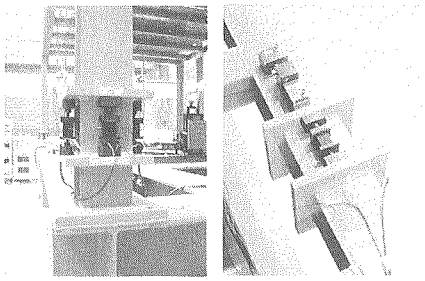

Figure 4 Piezoelectric actuators attached to column and beam

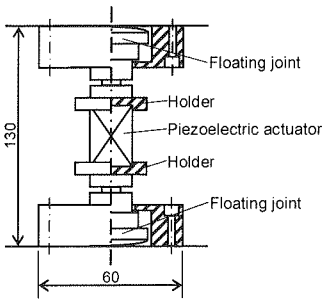

Figure 5 Installation method of piezoelectric actuator

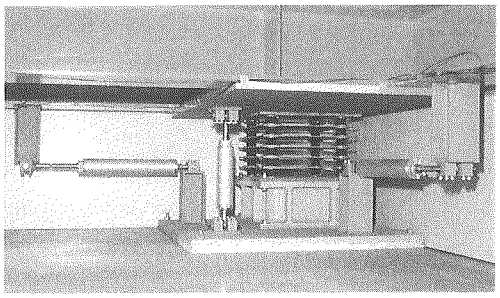

Figure 7 Piezoelectric actuator units installed in seismic isolation layer

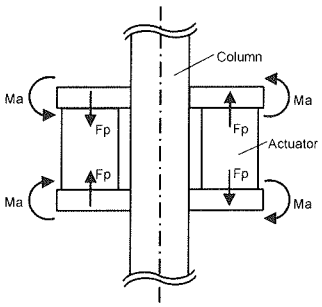

Figure 6 Bending moment control by piezoelectric actuators

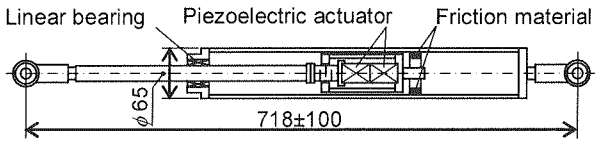

Figure 8 Schematic drawing of piezoelectric actuator unit

As shown in figure 7, four horizontal piezoelectric actuator units consisting of two piezoelectric actuators each and four vertical ones of the same type were installed between the bottom of the superstructure and the foundation. Figure 8 shows a schematic drawing of the piezoelectric actuator unit. The piezoelectric actuator units slide to protect the piezoelectric actuators when an earthquake occurs.

ANALYTICAL MODEL

In this study, the longitudinal, transverse and vertical directions in the building model were the x-direction, the y-direction and the z-direction respectively. Equations of motion based on the FEM analysis of the building model are written as follows:

$$[M]\{\ddot{X}\}+[K]\{X\}=-[M][H_z]\{\ddot{z}\}+[H_f]\{f\}+[H_w]\{w\}+[H_u]\{m_u\}+[H_v]\{f_v\} \quad (1)$$

where

$\{X\}=\{x_1\cdots x_n \quad y_1\cdots y_n \quad z_1\cdots z_n \quad \theta_{x1}\cdots\theta_{xn} \quad \theta_{y1}\cdots\theta_{yn} \quad \theta_{z1}\cdots\theta_{zn}\}^T$

: Vector of the displacements and the angles of rotation of each node

$\{\ddot{z}\}=\{\ddot{z}_x \quad \ddot{z}_y \quad \ddot{z}_z\}^T$: Vector of the ground accelerations

$\{f\}=\{f_x \quad f_y \quad f_z\}^T$: Vector of the excitation forces of the shakers installed in the center of the first floor

$\{w\}=\{w_x \quad w_y\}^T$: Vector of the excitation forces of the shakers installed in the center of the roof floor

$\{m_u\}=\{m_{u1} \quad m_{u2} \quad \cdots \quad m_{u20}\}^T$: Vector of the bending moments by the actuators attached to the columns and the beams

$\{f_v\}=\{f_{v1} \quad f_{v2} \quad \cdots \quad f_{v8}\}^T$: Vector of the forces by the actuator units installed in the seismic isolation layer

$[M]$: Matrix of mass and moment of inertia

$[K]$: Stiffness matrix

$[H_z]$: Coefficient matrix for the vector $\{\ddot{z}\}$

$[H_f]$: Coefficient matrix for the vector $\{f\}$

$[H_w]$: Coefficient matrix for the vector $\{w\}$

$[H_u]$: Coefficient matrix for the vector $\{m_u\}$

$[H_v]$: Coefficient matrix for the vector $\{f_v\}$

The vector $\{X\}$ is expressed by

$$\{X\}=[\phi]\{q\} \tag{2}$$

where $[\phi]$ and $\{q\}$ are the modal matrix and the vector of the modal displacements respectively. The modal matrix is normalized by

$$[\phi]^T[M][\phi]=[I] \tag{3}$$

Considering the modal damping, the modal equation of motion is obtained as

$$\{\ddot{q}\}+[2\zeta\omega]\{\dot{q}\}+[\omega^2]\{q\}=-[B_z]\{\ddot{z}\}+[B_f]\{f\}+[B_w]\{w\}+[B_u]\{m_u\}+[B_v]\{f_v\} \tag{4}$$

where

ζ : Modal damping ratio

ω : Natural frequency

$[B_z]$: Matrix of the participation factors concerning the vector $\{\ddot{z}\}$

$[B_f]$: Matrix of the participation factors concerning the vector $\{f\}$

$[B_w]$: Matrix of the participation factors concerning the vector $\{w\}$

$[B_u]$: Matrix of the participation factors concerning the vector $\{u\}$

$[B_v]$: Matrix of the participation factors concerning the vector $\{v\}$

Figure 9(a) shows six modes that were selected as the control objects when the piezoelectric actuator units were not installed. They were the fourth and sixth modes in which deformations of the columns in the y-direction were dominant, the fifth and tenth modes in which deformations of the columns in the x-direction were dominant, the eighth and fourteenth modes in which the second floor vibrated in the z-directions.

Figure 9(b) shows ten modes that were selected as the control objects when the piezoelectric actuator units were installed in the seismic isolation layer. They were the first, fourth and eighth modes in which deformations of the columns in the y-direction were dominant, the second, sixth and tenth modes in which deformations of the columns in the x-direction were dominant, the fifth, seventh and fourteenth modes in which the second or roof floor vibrated in the z-directions, the sixteenth mode in which the deformations of rubber bearings in the z-direction were dominant.

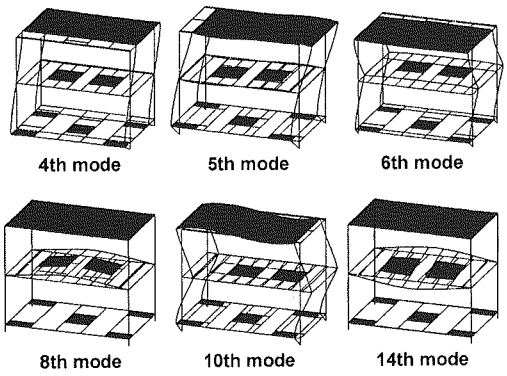

(a) Without piezoelectric actuator units

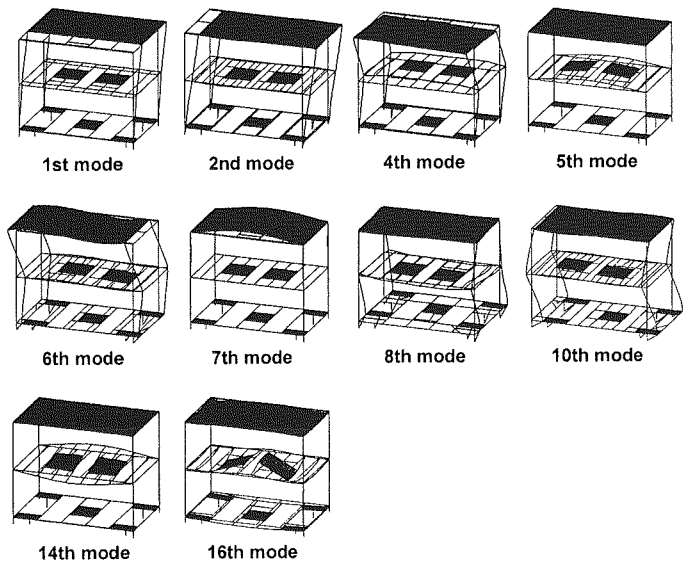

(b) With piezoelectric actuator units

Figure 9 Mode shapes of control objects

IDENTIFICATION OF MODAL PARAMETERS

The parameters of the analytical model were identified so as to obtain analytical results that are in good agreement with the experimental results in the following transfer functions in each direction.

(*a*) From the ground acceleration to the response accelerations of each floor

(*b*) From the excitation forces of the shakers to the response accelerations of each floor

(*c*) From the control voltages to the actuators attached to the columns and the beams to the response accelerations of each floor

(*d*) From the control voltages to the actuator units installed in the seismic isolation layer to the response accelerations of each floor

Excitation forces and the control voltages were generated from random noise in the frequency range of 1 to 30 Hz. Tables 1 and 2 show the results of the identification of natural frequencies and damping ratios.

Table 1 Modal parameters (Without piezoelectric actuator units)

Mode	Natural frequency [Hz]		Damping ratio [%]
	Exp.	Cal.	Cal.
4th	3.82	3.88	7.0
5th	5.42	5.44	5.0
6th	6.02	6.24	2.0
8th	7.47	7.49	0.1
10th	10.9	10.9	4.0
14th	18.3	21.5	0.5

Table 2 Modal parameters (With piezoelectric actuator units)

Mode	Natural frequency [Hz]		Damping ratio [%]
	Exp.	Cal.	Cal.
1st	2.50	2.42	1.3
2nd	3.48	3.43	1.3
4th	5.34	5.13	1.1
5th	7.51	7.06	0.5
6th	8.82	8.62	2.5
7th	9.82	9.88	0.5
8th	11.1	11.1	5.0
10th	12.4	12.7	5.0
14th	18.5	20.5	0.3
16th	23.5	22.8	1.0

DESIGN OF CONTROLLERS

The controllers were designed by a model-matching method [3]. Figure 10 shows a block diagram of the general control system, where u, y, v and d represent the control input, output, observation noise and disturbance respectively. From the block diagram, y is expressed as

$$y = P_{dy} d + P_{uy} u \tag{5}$$

where P_{dy} and P_{uy} are the open loop transfer functions of the plant from d to y, and from u to y, respectively. Since $u = C_{ru} r + C_{yu}(y + v)$, Eq. (5) is transformed to

$$y = (1 - P_{uy} C_{yu})^{-1} (P_{uy} C_{ru} r + P_{uy} C_{yu} v + P_{dy} d) \tag{6}$$

where C_{ru} and C_{yu} are the open loop transfer functions of the controller from r to u, and from y to u, respectively. Three closed loop transfer functions are defined by the following equations:

$$W_{ry} = (1 - P_{uy} C_{yu})^{-1} P_{uy} C_{ru} \tag{7}$$

$$W_{vy} = (1 - P_{uy} C_{yu})^{-1} P_{uy} C_{yu} \tag{8}$$

$$W_{dy} = (1 - P_{uy} C_{yu})^{-1} P_{dy} \tag{9}$$

where W_{ry}, W_{vy} and W_{dy} are the closed loop transfer functions from r to y, from v to y, and from d to y, respectively. From Eqs. (7), (8) and (9),

$$W_{dy} = (1 + W_{vy}) P_{dy} \tag{10}$$

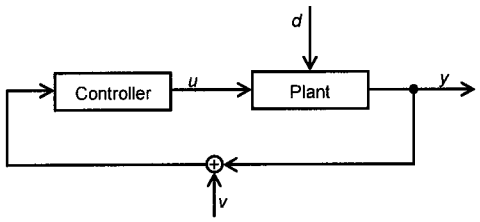

Figure 10 Block diagram of general control system

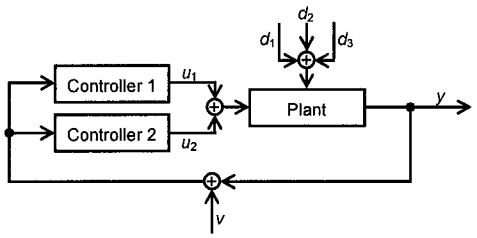

Figure 11 Block diagram of control system in this study

$$C_{yu} = P_{u_1y}^{-1} W_{vy} (1 + W_{vy})^{-1} \tag{11}$$

are obtained, where P_{dy} and P_{uy} are given. Therefore these equations mean that C_{yu} is uniquely determined by W_{vy} or W_{dy}.

The closed loop transfer function W_{vy} or W_{dy} is determined considering the following conditions:

(1) The transfer functions W_{vy} and W_{ry} must have larger relative orders than P_{uy}.
(2) The sets of zeros of W_{vy} and W_{ry} must contain all zeros of P_{uy}.
(3) The set of zeros of $(1+W_{ry})$ must contain all poles of P_{uy}.

These three conditions are conditions to obtain a proper controller.

Figure 11 shows a block diagram of the control system in this study, where u_1 and u_2 are the modal control inputs, d_1, d_2 and d_3 the modal disturbances, y is the modal output and v the observation noise. From the block diagram, y is expressed as

$$y = P_{d_1y} d_1 + P_{d_2y} d_2 + P_{d_3y} d_3 + P_{u_1y} u_1 + P_{u_2y} u_2 \tag{12}$$

In the control system, two modal control voltages were input to the plant (u_1 is the modal control voltage for the actuators attached to the columns and the beams and u_2 is for the actuator units installed in the seismic isolation layer), and three modal disturbances were input to the plant (d_1 by the shakers installed in the first floor, d_2 by the shaker installed in the roof floor and d_3 by ambient ground vibration). The controllers were designed independently. W_{d_1y}, W_{d_2y} and W_{d_3y} were chosen as follows:

$$W_{d_1y} = \frac{s^2(s^4 + \gamma_3 s^3 + \gamma_2 s^2 + \gamma_1 s + \gamma_0)}{(s-p_1)(s-p_2)\cdots(s-p_6)} \tag{13}$$

$$W_{d_2y} = \frac{s^2(s^4 + \gamma_3 s^3 + \gamma_2 s^2 + \gamma_1 s + \gamma_0)}{(s-p_1)(s-p_2)\cdots(s-p_6)} \tag{14}$$

$$W_{d_3y} = \frac{(2\zeta_i\omega_i s + \omega_i^2)(s^5 + \gamma_4 s^4 + \gamma_3 s^3 + \gamma_2 s^2 + \gamma_1 s + \gamma_0)}{(s-p_1)(s-p_2)\cdots(s-p_7)} \tag{15}$$

Then, the controller transfer functions C_{yu_1} and C_{yu_2} were calculated by

$$C_{yu_1} = P_{u_1y}^{-1} W_{vy} (1 + W_{vy})^{-1} = \frac{\beta_1 s^2 + \beta_0 s}{s^4 + \gamma_3 s^3 + \gamma_2 s^2 + \gamma_1 s + \gamma_0} \tag{16}$$

$$C_{yu_2} = P_{u_2y}^{-1} W_{vy} (1+W_{vy})^{-1} = \frac{\beta_2 s^3 + \beta_1 s^2 + \beta_0 s}{s^5 + \gamma_4 s^4 + \gamma_3 s^3 + \gamma_2 s^2 + \gamma_1 s + \gamma_0} \tag{17}$$

MICROVIBRATION CONTROL PERFORMANCES

Figure 12 shows fourier spectra of response accelerations due to wind conditions of actual base-isolated manufacturing facility in Iwata, Japan [4]. In the actual base-isolated manufacturing facility, only the first mode vibration was excited by the strong wind. Therefore, excitation forces of shaker installed in the roof floor to simulate the horizontal microvibrations excited by the wind were generated from the random noise which excite only the first mode.

Figure 13 shows the rms values of the response accelerations on the 1st floor, 2nd floor and roof floor in each direction. When the piezoelectric actuator units were not installed, the tests were carried out in cases when passive base-isolation with multistage rubber bearings and a viscous shear damper, controlled with the piezoelectric actuators attached to the columns and beams. The passive base-isolation system with the viscous shear damper could effectively reduce the horizontal microvibrations, but the system controlled with the piezoelectric actuators attached to the columns and the beams could more effectively reduce the three dimensional microvibrations. When the piezoelectric actuator units were installed, the tests were carried out in cases when non-controlled, controlled with the piezoelectric actuator units, controlled with all actuators. In these cases, microvibration reduction effects of the viscous shear damper were lost by installing the piezoelectric actuator units. Therefore, the response accelerations were reduced to 16-36% of those when non-controlled, but larger than when passive base-isolation. Thus, the system consisting of the passive base-isolation with the viscous shear damper and the piezoelectric actuators attached to the columns and the beams could most effectively control the three-dimensional microvibrations due to the external and the internal disturbances.

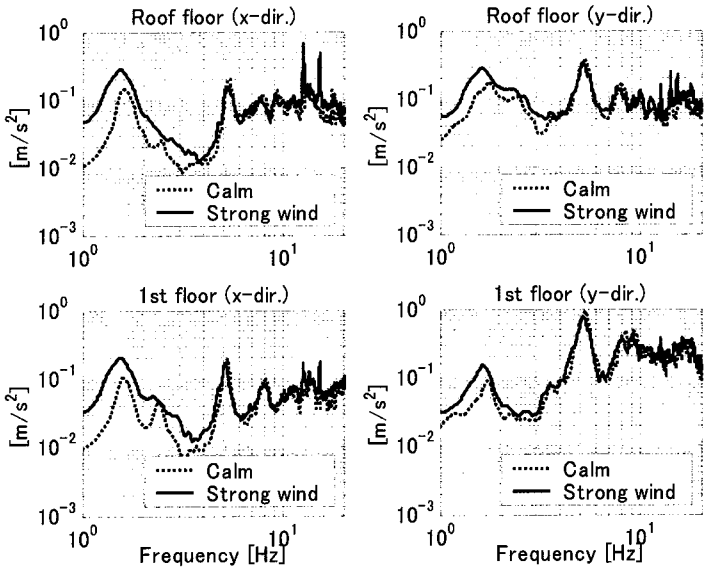

Fig. 12 Fourier spectra of response accelerations due to wind conditions of actual base-isolated manufacturing facility

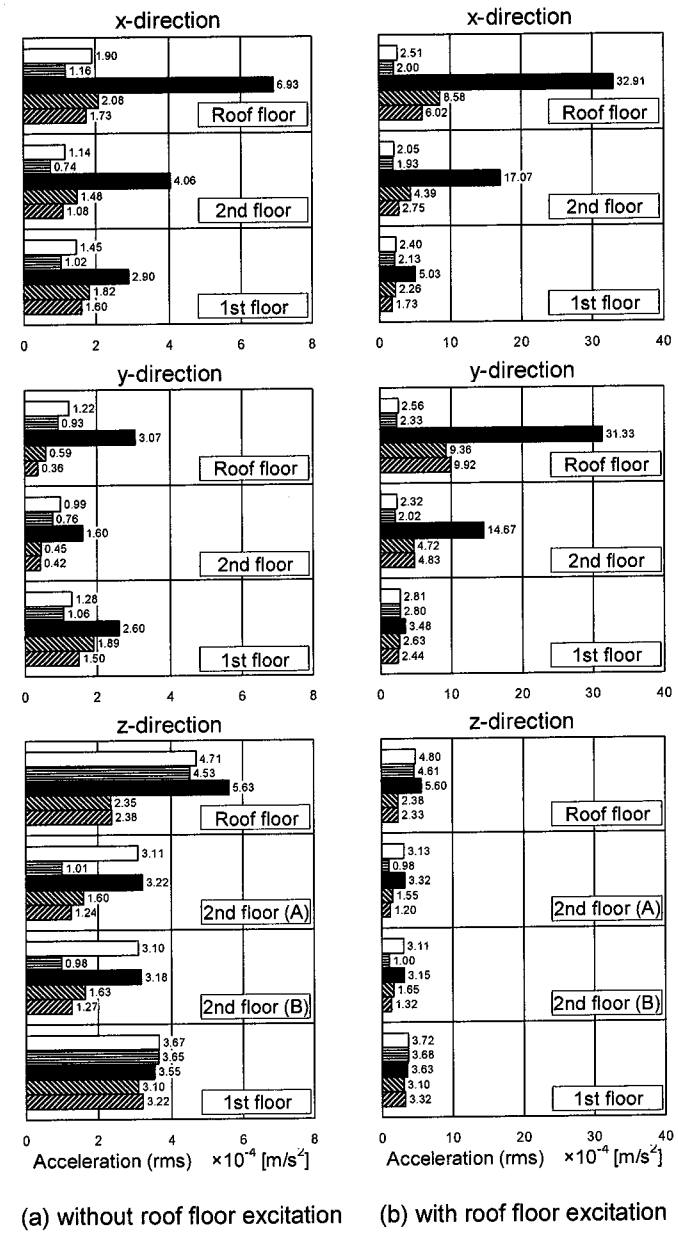

Figure 13 Rms values of response accelerations

CONCLUSION

In this study, the smart structure for the comprehensive active microvibration control systems of base-isolated precision manufacturing facilities were tested using the 2-story steel frame building model in which the piezoelectric actuators attached to the columns and the beams for the bending moment control of them, and four horizontal piezoelectric actuator units consisting of two piezoelectric actuators each and four vertical ones of the same type were installed between the bottom of the superstructure and the foundation. Through the tests, the system consisting of the passive base-isolation with the viscous shear damper and the piezoelectric actuators attached to the columns and the beams could most effectively control the three-dimensional microvibrations due to the external and the internal disturbances.

REFERENCES

1. T. Fujita, "Smart Structures for Active Vibration Control of Buildings," Proc. of the 1997 International Symposium on Active Control of Sound and Vibration (ACTIVE 97), pp. XIX-XXXIII, Budapest, Hungary, 1997
2. T. Kamada, T. Fujita, T. Hatayama, T. Arikabe, N. Murai, S. Aizawa, and K. Tohyama, "Active vibration control of frame structures with smart structures using piezoelectric actuators (Vibration control by control of bending moments of columns)," Smart Materials and Structures, Vol. 6, No. 4, pp. 448-456, 1997
3. T. Fujita, Y. Tagawa, N. Murai, S. Shibuya, A. Takeshita, and Y. Takahashi, "Study of Active Microvibration Control Device Using Piezoelectric Actuator (1st Report, Fundamental Study of One-Dimensional Microvibration Control)," Transactions of the Japan society of mechanical engineers, Vol. 57, No. 540, pp. 2560-2565, 1991 (in Japanese)
4. K. Yoshie, M. Asano, T. Erikawa, T. Matsuda, M. Yasuda, H. Kitamura, and T. Fujita, "Microvibration Characteristics of Base Isolated Buildings (Part 5 Measurements of Microvibration in a Base Isolated Factory under Strong Winds)," Summaries of Technical Papers of Annual Meeting Architectural Institute of Japan, B, Structures, Vol. II, pp. 561-562, 2002 (in Japanese)